Available online at www.sciencedirect.com
SCIENCE DIRECT®
C. R. Mecanique 332 (2004) 717–724
COMPTES RENDUS MECANIQUE

Reconstruction of the three mechanical material constants of a lossy fluid-like cylinder from low-frequency scattered acoustic fields

Thierry Scotti, Armand Wirgin *

Laboratoire de mécanique et d'acoustique, UPR 7051 du CNRS, 31, chemin Joseph Aiguier, 13402 Marseille cedex 20, France

Received 15 July 2003; accepted after revision 30 March 2004

Presented by Pierre Suquet

Abstract

The inverse medium problem for a circular cylindrical domain is studied using low-frequency acoustic waves as the probe radiation. To second order in k_0a (k_0 the wavenumber in the host medium, a the radius of the cylinder), only the first three terms (i.e., of orders 0, -1 and $+1$) in the partial wave representation of the scattered field are non-vanishing. This enables the scattered field to be expressed algebraically in terms of the unknown material constants, i.e., the density ρ_1, and the real and imaginary parts of complex compressibility κ_1 of the cylinder. It is shown that these relations can be inverted to yield explicit, decoupled expressions for ρ_1 and κ_1 in terms of the totality of the far-zone scattered field. These expressions furnish accurate estimations of the material parameters provided the probe frequency is low and the radius of the cylinder is known very precisely. ***To cite this article: T. Scotti, A. Wirgin, C. R. Mecanique 332 (2004).***

Résumé

Reconstruction des trois constants mécaniques matériels d'un cylindre fluide dissipatif à partir de champs acoustiques basses fréquences. Le problème inverse de milieu pour un domaine cylindrique circulaire est étudié en employant des ondes acoustiques comme rayonnement d'interrogation. Au second ordre en k_0a (k_0 le nombre d'onde dans le milieu-hôte et a le rayon du cylindre), seuls les trois premiers termes (i.e., les ordres 0, -1 and $+1$) dans le développement en ondes partielles du champ diffracté sont non-nuls. Ce fait permet d'exprimer le champ diffracté de manière algébrique en fonction des paramètres matériels que sont la densité ρ_1 et les parties réelle et imaginaire de la compressibilité complexe κ_1 du cylindre. On montre que ces relations peuvent être inversées afin de donner lieu à des expressions explicites et découplées pour ρ_1 and κ_1 en fonction de la totalité du champ diffracté en zone lointaine. Ces expressions fournissent des estimations précises des paramètres matériels à condition que la fréquence de sondage soit basse et le rayon du cylindre soit connu très précisément. ***Pour citer cet article : T. Scotti, A. Wirgin, C. R. Mecanique 332 (2004).***

Keywords: Acoustics; Inverse medium problem

* Corresponding author.
E-mail address: wirgin@lma.cnrs-mrs.fr (A. Wirgin).

1631-0721/$ – see front matter
doi:10.1016/j.crme.2004.03.018

Mots-clés : Acoustique ; Problème inverse de milieu

1. Introduction

Retrieving the mechanical material constants (e.g., elastic moduli, density) of a material, either by direct measurements of these quantities, or by measurements of other variables from which the material constants can be derived with the help of suitable models, is one of the central problems in material science. When the specimen is a solid, the elastic moduli are determined either by the usual static methods or by dynamic methods involving the inversion of data relative to resonant frequencies and/or mode shapes of vibrations excited, for instance by percussive forces [1–4], or relative to velocities and attenuations for ultrasonic wave probe radiation [5]. Ultrasound methods can also be employed for fluids, or fluid-like materials [5,6].

Another class of material characterization methods, called *resonance spectroscopy* [7] combines the underlying principles of vibratory resonances with an acoustic excitation of the specimen. This technique has also been employed to determine the refractive index of beads by means of laser irradiation [8]. This class of techniques differs from the previous ones in that it relies on measurements of the *wavefield diffracted by the specimen*, and appeals to a quite intricate theory relating the resonances to coefficients computed from the diffracted field for estimating the material parameters (it can also be employed for estimating the geometrical parameters of the specimen [7–9]). This theory is only feasible for specimens having simple geometry (e.g., spherical, circular cylindrical, plate-like). A simple specimen geometry is also required in the standard vibration-resonance and velocity-attenuation methods if absolute quantitative characterizations are aimed at.

During the last 25 years, another materials-characterization method has been developed which can be termed *wavefield imaging*. The underlying idea is: (i) acquire measurements of the field scattered from a specimen at a series of locations in space arising either from several monochromatic probe fields, and/or from a pulse-like probe field; and (ii) retrieve from these measurements an *image* of the specimen (i.e., a spatial map of some material characteristic, such as wavespeed or attenuation) with the help of a suitable model of the specimen/wave interaction. Insofar as there is a sharp difference between the material properties of the specimen and those of the host medium, this method also gives a picture of the geometry (location, orientation, size and shape) of the specimen. When, as is often the case, the reconstructed information relating to the material constants of the specimen is not reliable, only the reconstructed information of geometrical nature can been exploited (this is called *qualitative wavefield imaging*; otherwise it is called *quantitative wavefield imaging*). For instance, computerized diffraction tomography, making use of a model appealing either to the Rytov or Born approximations of the specimen/wave interaction, is a qualitative wavefield imaging technique except for specimens whose properties differ only slightly from those of the host medium (this is fortunately the case in biological imaging applications) [6,10–12]. It has been suggested [10–12] that one of the reasons why Born-based techniques do not furnish reliable estimates of the material properties (notably the wavespeed, in specimens assumed to be lossless and surrounded by a host medium which is also lossless and has the same density as that of the specimen), is that data relating to low-frequency probe radiation was either not available or not used in the inversion algorithm.

The importance of disposing of multi-frequency (and, in particular, low frequency) data is increasingly recognized as the key to success for material characterization in wavefield imaging techniques such as the distorted Born method [13,14], the modified Born and modified gradient methods [15], and the contrast source method [16]. The possibility of obtaining a quantitatively-accurate image with these iterative methods is often dependent on being able to initialize the algorithm with a plausible image of the object at the lowest frequency of the probe radiation. More often than not, this initial image is obtained via the Born approximation, and since the latter is not accurate for large contrasts (between the host and the object) of the material constants, the algorithm has trouble restoring the right values of the material constants during the iterative process. Thus, it would be useful to find a

means for obtaining a better estimate of the material constants at low frequencies in the case of contrasts that are not necessarily small. This is done herein.

In particular, we shall be concerned with the retrieval of the three material constants $\Re\kappa_1$, $\Im\kappa_1$ and ρ_1 (wherein $\kappa_1 = \Re\kappa_1 + \mathrm{i}\Im\kappa_1$) of a generally-lossy fluid-like object in a lossless fluid-like host probed by plane-wave acoustic radiation. The case $\Im\kappa_1 = 0$ of a lossless material can also be treated. No assumption is made concerning the contrasts of density and compressibility between the host and the object. The latter is assumed to be a circular cylinder, of known radius a. The material constants of the host medium (in which the probe radiation propagates) are also assumed to be known, as are known the frequency and incident angle of the plane wave probe radiation, as well as the scattered acoustic wavefield in the far zone of the cylinder. The analysis for recovering the three material parameters of the cylinder is focused on the case in which the wavelength ($\lambda_0 = 2\pi/k_0$, with $k_0 = \omega/c_0$, c_0 the velocity of bulk waves in the host, and ω the angular frequency) of the probe radiation is much larger than the cylinder radius.

2. Physical configuration and governing equations

The scattering body is an infinitely-long circular cylinder whose generators are parallel to the z axis in the cylindrical polar coordinate system (r, θ, z). The intersection of the cylinder (of radius a, whose center is located at the origin O), with the xOy plane defines (see Fig. 1):

(i) the boundary curve $\Gamma = \{r = a;\ 0 \leqslant \theta < 2\pi\}$;
(ii) the bounded (inner) region (i.e., that occupied by the body in its cross-section plane) $\Omega_1 = \{r < a;\ 0 \leqslant \theta < 2\pi\}$;
(iii) the unbounded (outer) region $\Omega_0 = \{r > a;\ 0 \leqslant \theta < 2\pi\}$.

It is assumed that Ω_0 and Ω_1 are filled with linear, homogeneous, isotropic, time-invariant fluid-like media M_0 and M_1 respectively and that M_1 is possibly lossy. The (generally-complex) bulk wave velocity c_j in M_j is related to the (real) density ρ_j and (generally-complex) compressibility κ_j by $c_j = (\rho_j \kappa_j)^{-1/2}$.

The cylinder is probed by a monochromatic acoustic plane wave whose propagation vector lies in the xOy plane. Due to the invariance of the cylinder and incident field with respect to z, the scattered and total fields are

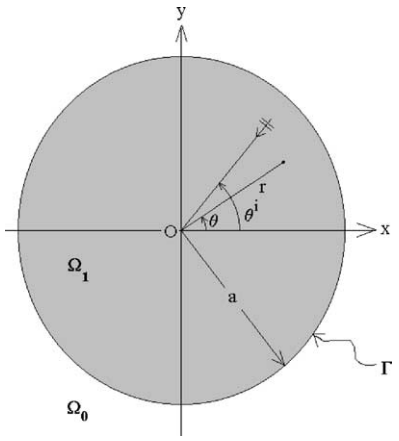

Fig. 1. Problem configuration in the xOy plane.

also invariant with respect to z. Let U designate pressure, which, due to the previously-mentioned invariance, is of the form:

$$U = U(\mathbf{x}, t) \tag{1}$$

with $\mathbf{x} = (x, y) = (r, \theta)$. This invariance applies also when superscripts i and d (i for 'incident' and d for 'diffracted') are attached to U. It is convenient to associate $U(\mathbf{x}, t)$ with the total field, it being understood that the latter takes the form $U_j(\mathbf{x}, t)$ in Ω_j and:

$$U_j(\mathbf{x}, t) = U^i(\mathbf{x}, t)\delta_{j0} + U_j^d(\mathbf{x}, t); \quad \mathbf{x} \in \Omega_j \tag{2}$$

with δ_{jk} the Kronecker delta.

We express U by the Fourier transform

$$U_j(\mathbf{x}, t) = \int_{-\infty}^{\infty} u_j(\mathbf{x}, \omega) \exp(-\mathrm{i}\omega t)\, \mathrm{d}\omega \tag{3}$$

with similar expressions for U^i and U^d. The monochromatic, plane-wave nature of the incident field is such that

$$u^i(\mathbf{x}, \omega) = \exp\bigl[-\mathrm{i}k_0 r \cos\bigl(\theta - \theta^i\bigr)\bigr] \tag{4}$$

wherein θ^i designates the incident angle.

The essential task in both the forward and inverse scattering contexts is to determine

$$u_j(\mathbf{x}, \omega) = u^i(\mathbf{x}, \omega)\delta_{j0} + u_j^d(\mathbf{x}, \omega); \quad \mathbf{x} \in \Omega_j \tag{5}$$

3. Forward and inverse scattering problems

The *forward scattering problem* (notably for simulating measured data) is formulated as follows. Given: (i) the location, shape, size and composition (material properties) of the scattering body; (ii) the material properties of the host medium M_0; (iii) the incident wavefield (i.e., (4)), as well as the frequency thereof, determine: the field (i.e., u_j^d; $j = 0, 1$) scattered by the body at arbitrary points of space.

The general *inverse scattering problem* is formulated as follows. Given: (i) the incident wavefield, as well as the frequency thereof; (ii) the material properties of the host medium M_0; (iii) the wavefield in some subregion of Ω_0, reconstruct: the location, shape, size and composition of the scattering body.

Hereafter, we shall be concerned mostly with the *inverse problem*, and, in particular, with one in which *the location, size and shape of the body are known beforehand* (*actually, the size will be determined by measurement*), the task being to *reconstruct the composition of the body*, embodied in its material properties ρ_1 and κ_1, from the scattered acoustic field in the far zone for *low-frequency probe radiation*.

4. Partial wave expressions of the fields

The plane-wave probe radiation admits the partial wave expansion [17]

$$u^i(\mathbf{x}, \omega) = \sum_{m=-\infty}^{\infty} \gamma_m J_m(k_0 r) \exp(\mathrm{i}m\theta); \quad \forall \mathbf{x} \in \mathbb{R}^2 \tag{6}$$

wherein $J_m(\cdot)$ is the mth order Bessel function and

$$\gamma_m = \exp\bigl(-\mathrm{i}m\bigl(\theta^i + \pi/2\bigr)\bigr) \tag{7}$$

Similarly,

$$u_0^d(\mathbf{x},\omega) = \sum_{m=-\infty}^{\infty} C_m H_m^{(1)}(k_0 r)\exp(\mathrm{i}m\theta); \quad \forall \mathbf{x} \in \Omega_0 \tag{8}$$

wherein $H_m^{(1)}(\cdot)$ is the mth order Hankel function, and, on account of the continuity of pressure and the normal component of particle velocity across Γ,

$$C_m = \gamma_m \frac{J_m(k_0 a)\dot{J}_m(k_1 a) - \beta \dot{J}_m(k_0 a) J_m(k_1 a)}{\beta \dot{H}_m^{(1)}(k_0 a) J_m(k_1 a) - H_m^{(1)}(k_0 a)\dot{J}_m(k_1 a)} \tag{9}$$

with: $Z_m(\xi) = J_m(\xi)$, $Z_m(\xi) = Y_m(\xi)$ or any linear combination thereof, knowing that $H_m^{(1)}(\xi) = J_m(\xi) + \mathrm{i}Y_m(\xi)$, with $Y_m(\xi)$ the mth order Neumann function), $\dot{Z}(\xi) := \mathrm{d}Z(\xi)/\mathrm{d}\xi$ and $\beta = k_0\rho_1/k_1\rho_0$.

It is customary, but not necessary, to measure the field in the far zone. In this case, we employ the large-argument asymptotic form of the Hankel functions [17] to obtain

$$u_0^d(\mathbf{x},\omega) \sim \breve{u}_0^d(\theta,\theta^i,\omega)\sqrt{\frac{2}{\pi k_0 r}}\exp\left[\mathrm{i}\left(k_0 r - \frac{\pi}{4}\right)\right]; \quad k_0 r \to \infty \tag{10}$$

wherein, the so-called *far-field scattering function* is given by

$$\breve{u}_0^d(\theta,\theta^i,\omega) = \sum_{m=-\infty}^{\infty} C_m \exp\bigl[\mathrm{i}m(\theta - \pi/2)\bigr] \tag{11}$$

5. Low-frequency approximation of the scattered field outside of the body and inversion formulas

We make the hypothesis of low frequencies (and/or small cylinder radius),

$$k_0 a \ll 1 \tag{12}$$

and employ a second order in $k_0 a$ perturbation scheme to obtain, with the help of the small-argument asymptotic forms of the Bessel and Neumann functions [17],

$$u_0^d(\mathbf{x},\omega) \sim \frac{\mathrm{i}\pi(k_0 a)^2}{4}\left[\left(\frac{\kappa_1}{\kappa_0} - 1\right)H_0^{(1)}(k_0 r) - 2\mathrm{i}\left(\frac{\rho_1/\rho_0 - 1}{\rho_1/\rho_0 + 1}\right)H_1^{(1)}(k_0 r)\cos\bigl(\theta - \theta^i\bigr)\right]$$
$$\forall \mathbf{x} \in \Omega_0; \quad k_0 a \to 0 \tag{13}$$

$$\breve{u}_0^d(\theta,\theta^i,\omega) \sim \frac{\mathrm{i}\pi(k_0 a)^2}{4}\left[\left(\frac{\kappa_1}{\kappa_0} - 1\right) - 2\left(\frac{\rho_1/\rho_0 - 1}{\rho_1/\rho_0 + 1}\right)\cos\bigl(\theta - \theta^i\bigr)\right]; \quad k_0 a \to 0 \tag{14}$$

(note that in [18], the reader is asked to demonstrate (14)). The general problem in (13) and (14) is to express A and B in terms of $C(\theta)$; $\forall \theta \in [0, 2\pi[$ knowing that

$$C(\theta) = A + B\cos\bigl(\theta - \theta^i\bigr); \quad \forall \theta \in [0, 2\pi[\tag{15}$$

We easily find:

$$A = \frac{1}{2\pi}\int_0^{2\pi} C(\theta)\,\mathrm{d}\theta, \qquad B = \frac{1}{\pi\cos\theta^i}\int_0^{2\pi} C(\theta)\cos\theta\,\mathrm{d}\theta \tag{16}$$

Applied to (14), this gives:

$$\kappa_1 = \kappa_0\left[1 + \frac{4}{\mathrm{i}\pi(k_0a)^2}\frac{1}{2\pi}\int_0^{2\pi} \breve{u}_0^d(\theta,\theta^i,\omega)\,\mathrm{d}\theta\right], \tag{17}$$

$$\rho_1 = \rho_0\left[\frac{1 - 2/(\mathrm{i}\pi(k_0a)^2)1/(\pi\cos\theta^i)\int_0^{2\pi}\breve{u}_0^d(\theta,\theta^i,\omega)\cos\theta\,\mathrm{d}\theta}{1 + 2/(\mathrm{i}\pi(k_0a)^2)1/(\pi\cos\theta^i)\int_0^{2\pi}\breve{u}_0^d(\theta,\theta^i,\omega)\cos\theta\,\mathrm{d}\theta}\right] \tag{18}$$

This shows that: (i) κ_1 can be retrieved independently of ρ_1; (ii) κ_1 is a linear function of the measured far zone scattered field; whereas (iii) ρ_1 is a nonlinear function of this field. More importantly: (17) and (18) constitute a method for determining ρ_1 and the real and imaginary parts of κ_1 from the (far-field) scattering function, in an explicit, analytic manner.

6. Numerical results

We applied formulas (17) and (18) to retrieve the density and complex compressibility from the far-field scattering function, assuming that the radius a was obtained beforehand by an appropriate measurement procedure. In particular, we computed the relative errors (see Figs. 2 and 3):

$$\delta_{\rho_1} := \left|\frac{\tilde{\rho}_1 - \rho_1}{\rho_1}\right|, \quad \delta_{\Re\kappa_1} := \left|\frac{\Re\tilde{\kappa}_1 - \Re\kappa_1}{\Re\kappa_1}\right|, \quad \delta_{\Im\kappa_1} := \left|\frac{\Im\tilde{\kappa}_1 - \Im\kappa_1}{\Im\kappa_1}\right| \tag{19}$$

(wherein ρ_1, κ_1, are the actual values of density and compressibility (i.e., those employed in generating the data), and $\tilde{\rho}_1$ is the value of density obtained from (18), while $\Re\tilde{\kappa}_1$, $\Im\tilde{\kappa}_1$ are the values of the real and imaginary parts of the complex compressibility obtained from (17)) over a range of frequencies corresponding to $10^{-5} \leqslant k_0a \leqslant 1.0$. The far-field data was simulated using (11) in which the lower and upper limits of the series were replaced by -5 and $+5$ respectively and use was also made of (10). The other parameters involved in the production of this data were: $\theta^i = 0$, $\rho_0 = 1000$ kg/m^3, $c_0 = 1500$ m/s, $\rho_1 = 1200$ kg/m^3, with $c_1 = 1600 + \mathrm{i}160$ m/s for the so-called low-contrast cylinder and $c_1 = 2500 + \mathrm{i}250$ m/s for the so-called high-contrast cylinder.

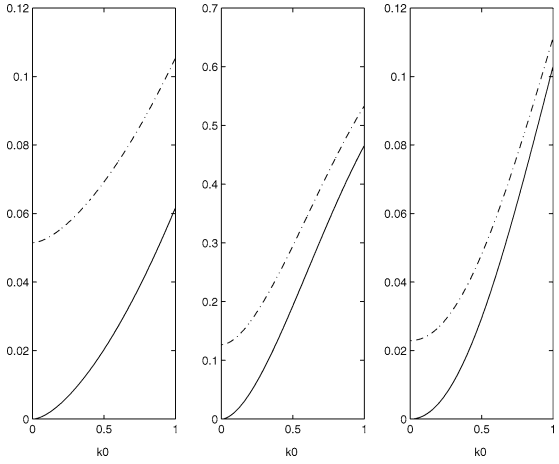

Fig. 2. Relative error of $\Re\kappa_1$ (left panel), $\Im\kappa_1$ (middle panel) and ρ_1 (right panel) as a function of wavenumber k_0 (note that k_0 increases linearly with frequency) for the relatively-low contrast cylinder. The continuous line curves apply to the exact radius case whereas the discontinuous line curves apply to the error-ridden radius case.

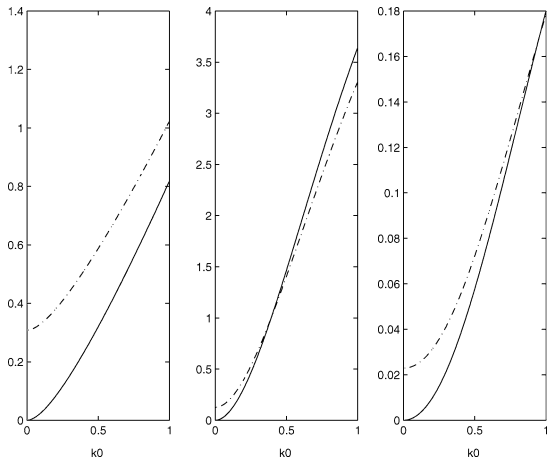

Fig. 3. Relative error of $\Re\kappa_1$ (left panel), $\Im\kappa_1$ (middle panel) and ρ_1 (right panel) as a function of wavenumber k_0 for the relatively-high contrast cylinder. Same notations as in Fig. 2.

To test the sensitivity of the method to cylinder radius measurement error, the reconstruction of $\tilde{\rho}_1$, $\Re\tilde{\kappa}_1$, $\Im\tilde{\kappa}_1$ was made in two cases: (i) using in (17) and (18) the exact value (1 m) for the radius a (i.e., zero measurement error of this parameter); and (ii) using in (17) and (18) an error-ridden value (1.07 m) for the radius (i.e., 7% measurement error for a). Note that in both cases, the computation via (11) of the data pertaining to the far-zone scattering function was carried out assuming the exact value $a = 1$ m for the radius.

One sees from Fig. 2 (solid curves) that in order to get relative errors of all three mechanical material parameters of the low-contrast cylinder inferior or equal to 10%, the probe frequency should be such that $k_0 a$ is not greater than ~ 0.35 provided the measurement of a is free of error.

One observes in the same figure (discontinuous curves) that when the error-ridden radius is introduced into the inversion computation, employing frequencies such that $k_0 a$ is not greater than ~ 0.35 results in relative errors in all three mechanical material parameters that can be as large as 23%.

In Fig. 3 one sees (solid curves) that the radius error has a relatively-smaller effect in the high-contrast cylinder case, but in order to obtain relative errors of all three mechanical material parameters inferior to 10%, $k_0 a$ must not exceed ~ 0.1 when the exact value of the radius is employed, and no frequency, however small, will enable to obtain reconstructions with less than 10% error by use of the error-ridden radius.

7. Conclusion

The asymptotic method for low frequency probe radiation is interesting in that it provides solutions to the inverse medium problem which can be written in *closed form* and are *unique* (recall that non-uniqueness is an oft-encountered feature of inverse medium problems [19]). Moreover, these solutions do not rely (as those appealing to the Born approximation) on the assumption of low bulk velocity and density contrasts. However, for a given operating frequency, the error of the asymptotic low frequency reconstructions has been found to increase with the velocity contrast. This can be overcome by employing lower frequencies for higher-contrast cylinders.

Radius measurement error appears to have less effect on the error of reconstructions for higher- than for lower-contrast cylinders. Whatever the contrast of material parameters, the effect of radius measurement error on the accuracy of the reconstructions is found to be relatively large, which means that the unstable nature [19] of material parameter reconstruction is not fundamentally modified by the advantage of being able to carry out the reconstruction in closed form.

The asymptotic solutions of the inverse problem obtained with low-frequency probe radiation should provide suitable starting solutions for reconstructions carried out with higher-frequency probe radiation as well as possible explanations of the difficulties encountered in inverse medium problems such as the one considered herein. They may also provide decent estimates of the material parameters of homogeneous (and even inhomogeneous) bodies of more general shapes.

The method outlined herein is transposable to other canonical bodies: homogeneous fluid slabs and spheres, homogeneous elastic slabs, circular cylinders and spheres, and to fluid-like or elastic circular tubes and spherical shells.

References

[1] P. Cawley, R.D. Adams, Vibration techniques, in: J. Summerscales (Ed.), Non-Destructive Testing of Fibre-Reinforced Plastics Composites, vol. 1, Elsevier, London, 1987, pp. 151–205.

[2] A. Vary, Acousto-ultrasonics, in: J. Summerscales (Ed.), Non-Destructive Testing of Fibre-Reinforced Plastics Composites, vol. 2, Elsevier, London, 1990, pp. 1–54.

[3] J.E. Grady, B.A. Lerch, Effect of heat treatment on stiffness and damping of SIC/Ti-15-3, in: P.K. Raju (Ed.), Vibro-Acoustic Characterization of Materials and Structures, in: NCA, vol. 14, ASME, New York, 1992, pp. 13–20.

[4] M.F. Nelson, J.A. Wolf Jr., A nondestructive technique for determining the elastic constants of advanced composites, in: P.K. Raju (Ed.), Vibro-Acoustic Characterization of Materials and Structures, in: NCA, vol. 14, ASME, New York, 1992, pp. 227–233.

[5] J. Krautkramer, H. Krautkramer, Ultrasonic Testing of Materials, Springer, New York, 1969.
[6] B.S. Robinson, J.F. Greenleaf, The scattering of ultrasound by cylinders: implications for diffraction tomography, J. Acoust. Soc. Am. 80 (1986) 40–49.
[7] J.D. Alemar, P.P. Delsanto, E. Rosario, Spectral analysis of the scattering of acoustic waves from a fluid cylinder. III. Solution of the inverse scattering problem, Acustica 61 (1986) 14–20.
[8] P. Chylek, V. Ramaswamy, A. Ashkin, J.M. Dziedzic, Simultaneous determination of refractive index and size of spherical dielectric particles from light scattering data, Appl. Opt. 22 (1983) 2302–2307.
[9] A.K. Datta, S.C. Som, On the inverse scattering problem for dielectric cylindrical scatterers, IEEE Trans. Anten. Prop. 29 (1981) 392–397.
[10] W. Tobocman, In vivo biomicroscopy with ultrasound, Current Topics in Acoust. Res. 1 (1994) 247–265.
[11] S. Delamare, J.-P. Lefebvre, P. Lasaygues, Back scattered ultrasonic tomography: experiments and modelizations, in: S. Lees, L.A. Ferrari (Eds.), Acoustical Imaging, vol. 23, Plenum Press, New York, 1997, pp. 595–600.
[12] S. Delamare, Sur l'approximation de Born dans la tomographie ultrasonore, Doctoral thesis, Université Aix-Marseille II, Marseille, 1999, pp. 62–64.
[13] O.S. Haddadin, E.S. Ebbini, Multiple frequency distorted Born iterative method for tomographic imaging, in: S. Lees, L.A. Ferrari (Eds.), Acoustical Imaging, vol. 23, Plenum Press, New York, 1997, pp. 613–619.
[14] A.G. Tijhuis, K. Belkebir, A.C.S. Litman, B.P. de Hon, Multiple-frequency distorted-wave Born approach to 2D inverse profiling, Inverse Problems 17 (2001) 1635–1644.
[15] K. Belkebir, A.G. Tijhuis, Modified gradient method and modified Born method for solving a two-dimensional inverse scattering problem, Inverse Problems 17 (2001) 1671–1688.
[16] R.F. Bloemenkamp, A. Abubakar, P.M. van de Berg, Inversion of experimental multi-frequency data using the contrast source inversion method, Inverse Problems 17 (2001) 1611–1622.
[17] M. Abramowitz, A. Stegun, Handbook of Mathematical Functions, Dover, New York, 1968.
[18] P.M. Morse, K.U. Ingard, Theoretical Acoustics, McGraw-Hill, New York, 1968, p. 464.
[19] H.D. Bui, Introduction aux Problemes Inverses en Mécanique des Materiaux, Eyrolles, Paris, 1993.